# Study on Absence of Room-Temperature Ferromagnetism in the Mn-AlN Films With Various Mn Concentrations



doi: 10.1109/TMAG.2008.2002366

# Study on Absence of Room-Temperature Ferromagnetism in the Mn-AlN Films With Various Mn Concentrations

Takanobu Sato[1], Yasushi Endo[2], Yoshio Kawamura[1], Fumiyoshi Kirino[3], Ryoichi Nakatani[1], and Masahiko Yamamoto[1]

[1]Department of Materials Science and Engineering, Graduate School of Engineering, Osaka University, Osaka 565-0871, Japan
[2]Department of Electrical and Communication Engineering, Graduate School of Engineering, Tohoku University, Sendai 980-8579, Japan
[3]Conservation of Cultural Property, Graduate School of Fine Arts, Tokyo National University of Fine Arts and Music, Tokyo 110-8714, Japan

**We have investigated the magnetic behavior and structure of polycrystalline Mn-AlN ($Al_{1-x}Mn_xN$) films with various Mn concentrations ($x = 0.05$–$0.24$) fabricated by reactive direct current (dc) magnetron sputtering. The magnetic behavior of these films depends on the Mn concentration $x$. The films with $x = 0.05$–$0.10$ show a paramagnetic behavior at 10–300 K. The film with $x = 0.17$ shows remanent magnetization and coercivity only at 10 K, while that with $x = 0.24$ shows an unknown magnetic behavior. Only würtzite-type AlN phase is observed for $x$ below 0.10. The coexistence of a würtzite-type AlN phase and a secondary phase such as Al–Mn alloy, Mn-nitride, or Al–Mn–N ternary compound is observed for $x = 0.17$. The coexistence of a würtzite-type AlN phase and a $ThH_2$-type $Mn_3N_2$ phase is observed for $x = 0.24$. From these results, it is concluded that the $Al_{1-x}Mn_xN$ films do not exhibit room-temperature (RT) ferromagnetism for all $x$. Moreover, it is likely that the ferromagnetic behavior observed at 10 K for $x = 0.17$ is caused by the secondary phase.**

*Index Terms*—**Magnetic semiconductors, Mn-AlN films, paramagnetic behavior, room-temperature (RT) ferromagnetism.**

## I. Introduction

DILUTED magnetic semiconductors (DMSs) have attracted much attention as the materials for spin electronics. In particular, InAs and GaAs doped with Mn exhibit carrier-induced ferromagnetism [1], [2], and their ferromagnetic properties can be controlled by an electric field [3] or light illumination [4], [5]. Many groups have investigated these DMSs from fundamental and technological points of view. However, it is difficult to apply these DMSs to electric devices that operate at room temperature (RT), because their Curie temperatures are much lower than RT [6]. Thus, discovering DMSs with ferromagnetism at RT is an important subject.

Recently, it has been reported that nitride semiconductors doped with Mn fabricated by reactive sputtering and molecular beam epitaxy exhibit ferromagnetism, and the Curie temperature is above 300 K for Mn-AlN [7], [8] and 940 K for Mn–GaN [9]. Some groups have suggested that these Mn-doped nitride semiconductors are one of the candidate materials for devices operating above RT. On the other hand, other groups have suggested that these materials do not exhibit ferromagnetism at RT [10], [11]. Thus, whether these materials exhibit ferromagnetism above RT remains to be elucidated. However, clear evidence of ferromagnetism above RT in these materials is yet to be reported.

In this study, we have investigated the magnetic behavior and structure of Mn-AlN ($Al_{1-x}Mn_xN$: $x = 0.05$–$0.24$) films fabricated by reactive direct current (dc) magnetron sputtering, and report the absence of ferromagnetism at RT in these films. In addition, we discuss the origin of magnetic behavior in these films from the structural point of view.

Digital Object Identifier 10.1109/TMAG.2008.2002366

## II. Experimental Procedure

Mn-AlN ($Al_{1-x}Mn_xN$) films were fabricated using reactive dc magnetron sputtering onto thermally oxidized Si (100) substrates at room temperature. The base pressure was better than $9 \times 10^{-7}$ Pa. The pressure of the Ar and $N_2$ gas mixture was maintained at 0.5 Pa and the mixture ratio was 1 : 1. The film thickness was either 50 or 250 nm. The Mn concentration $x$ was varied from 0.05 to 0.24. The Mn concentration was measured by energy-dispersive X-ray analysis (EDX).

The magnetization of these films was measured using a superconducting quantum interference device (SQUID) magnetometer with a maximum field of 50 kOe in the temperature range of 10–300 K. The magnetic field was applied along several directions in the film plane and a direction perpendicular to the film plane to confirm magnetic anisotropy. The measured magnetization contained the diamagnetism of the thermally oxidized Si (100) substrate in addition to the magnetism of the $Al_{1-x}Mn_xN$ films. We estimated the magnetization of the $Al_{1-x}Mn_xN$ films by subtracting the diamagnetism of the thermally oxidized Si (100) substrate. The structure of $Al_{1-x}Mn_xN$ films was investigated by grazing-incidence X-ray diffraction with an incidence angle of 0.5° using Cu–K$\alpha$ radiation, and transmission electron microscopy (TEM).

## III. Results and Discussion

Fig. 1 shows the in-plane magnetization curves at 10 and 300 K for 250-nm-thick $Al_{1-x}Mn_xN$ films with various Mn concentrations $x$. Similar magnetization curves are observed along several directions in the film plane and a direction perpendicular to the film plane at 10 K (it is not shown here). This reveals that these films do not show any obvious anisotropy in the film plane and perpendicular to the film plane. The magnetization curves at 300 K do not show a remanent magnetization and coercivity for all $x$. Furthermore, the magnetization

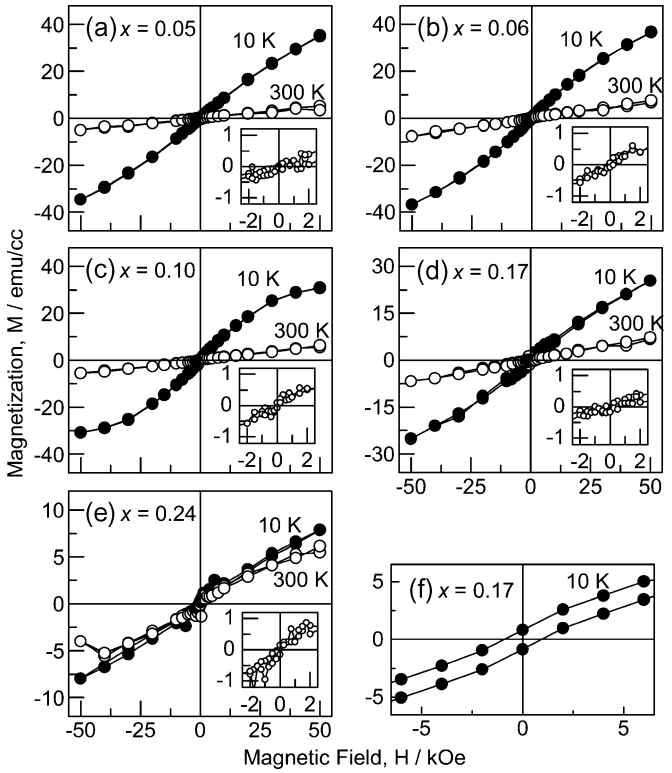


Fig. 1. (a)–(e) In-plane magnetization curves at 10 and 300 K for 250-nm-thick $Al_{1-x}Mn_xN$ films with various Mn concentrations. (f) Enlargement of magnetization curve at 10 K for $x = 0.17$.

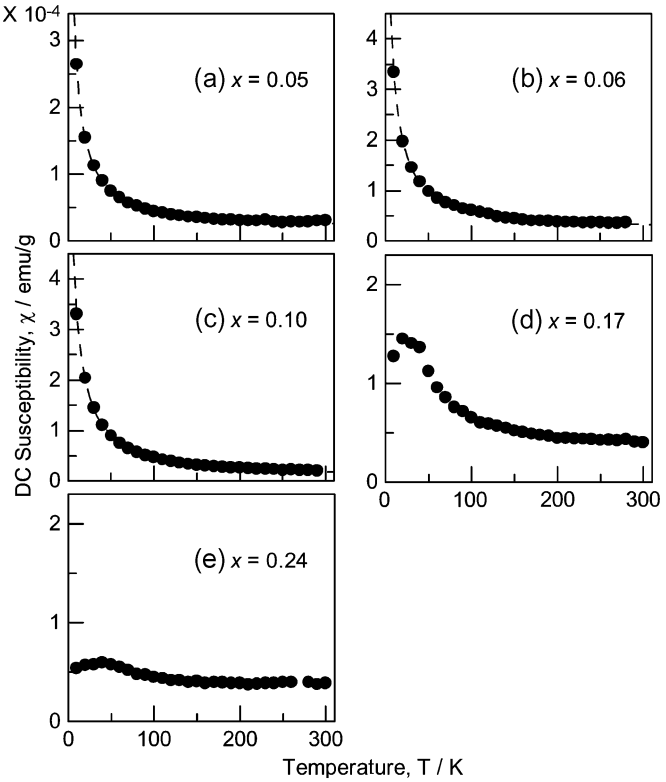


Fig. 2. Temperature dependence of dc susceptibility for 250-nm-thick $Al_{1-x}Mn_xN$ films with various Mn concentrations.

linearly increases with increasing magnetic field and no sharp change of magnetization is observed near zero magnetic field (see inset of Fig. 1). If these films contain ferromagnetic contribution that should show higher susceptibility than paramagnetic one before saturation, sharp change of magnetization near zero field should appear. Therefore, these observations reveal that the $Al_{1-x}Mn_xN$ films do not exhibit ferromagnetism at 300 K for all $x$. The magnetization curves at 10 K vary with $x$. In the range of $x = 0.05$–$0.10$, the remanent magnetization and coercivity are not confirmed and the magnetization does not saturate at a magnetic field of 50 kOe. These results show that $Al_{1-x}Mn_xN$ films do not exhibit ferromagnetism at 10 K for this range of $x$. For $x = 0.17$, remanent magnetization and coercivity are observed, which are 0.8 emu/cc and 0.9 kOe, respectively [see Fig. 1(f)]. However, the magnetization does not saturate at a magnetic field of 50 kOe. Thus, this magnetic behavior cannot be considered as a simple ferromagnetic behavior. This type of magnetization curve can be explained by a mix of ferromagnetic and paramagnetic behavior or a weak ferromagnetism observed in some antiferromagnet [12]. Furthermore, similar to those for $x = 0.05$–$0.10$, the remanent magnetization and coercivity are not observed for $x = 0.24$, and the magnetization does not saturate at a magnetic field of 50 kOe. Moreover, the magnetization of this film is lower than that of the films below $x = 0.17$. This reveals that the $Al_{1-x}Mn_xN$ film does not exhibit ferromagnetism at 10 K for $x = 0.24$.

To more precisely investigate the magnetic behavior of the $Al_{1-x}Mn_xN$ films, we measured the temperature dependence of dc susceptibility at a magnetic field of 10 kOe. The results are shown in Fig. 2. The dc susceptibility nearly corresponds to the initial susceptibility because the magnetization curves at 10 and 300 K (Fig. 1) are almost linear in the magnetic field range of $\pm 10$ kOe, except for the magnetization curve of the $Al_{0.83}Mn_{0.17}N$ film at 10 K. In the $x$ range of 0.05–0.10, the dc susceptibility markedly deceases with increasing temperature. This behavior is considered to obey Curie–Weiss law because these curves can be fitted by inversely proportional function (shown as broken line). This reveals that the magnetic behavior of the $Al_{1-x}Mn_xN$ films is paramagnetic for $x = 0.05$–$0.10$ in the temperature range of 10–300 K. For $x = 0.17$, the dc susceptibility increases with increasing temperature up to 20 K. This behavior excludes the possibility of a mix of ferromagnetic and paramagnetic behavior because the dc susceptibility of these magnetic behaviors does not increase with increasing temperature. The dc susceptibility decreases with increasing temperature above 20 K for $x = 0.17$. This suggests that the magnetic behavior of the film becomes paramagnetic above 20 K. Furthermore, for $x = 0.24$, the dc susceptibility increases up to 40 K and decreases above 40 K. However, the dc susceptibility is relatively low and the change in dc susceptibility with temperature is small. Therefore, the magnetic behavior of the film with $x = 0.24$ cannot be determined using only the results from this study.

Fig. 3 shows the grazing-incidence X-ray diffraction profiles of 250-nm-thick $Al_{1-x}Mn_xN$ films with various Mn concentrations $x$. In the range of $x$ below 0.17, the diffraction peaks are observed around the diffraction angles $2\theta$ of 35.9°, 65.6°, 94.4°, and 125.5°, which are derived from würtzite-type AlN

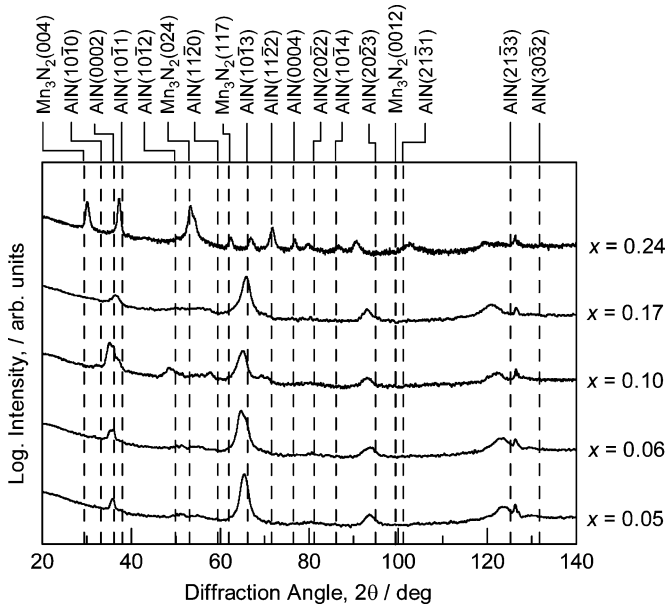


Fig. 3. Grazing-angle X-ray diffraction profiles of 250-nm-thick $Al_{1-x}Mn_xN$ films with various Mn concentrations. Broken lines denote the peak positions of bulk würtzite-type AlN and bulk $ThH_2$-type $Mn_3N_2$.

$(0002)$, $(10\bar{1}3)$, $(20\bar{2}3)$, and $(21\bar{3}3)$, respectively. The peak positions change with $x$. In addition to these peaks, for $x = 0.06$, a diffraction peak is observed around the diffraction angle $2\theta$ of 50.5°, which is derived from würtzite-type AlN $(10\bar{1}2)$. For $x = 0.24$, other diffraction peaks are also observed at $2\theta = 30.1°$, 53.3°, 62.3°, and 102.6°, which are derived from $ThH_2$-type $Mn_3N_2$ $(004)$, $(024)$, $(117)$, and $(0012)$, respectively. Therefore, the film with $x = 0.24$ includes a secondary phase.

To observe the structures more precisely, TEM was utilized. Fig. 4 shows selected-area diffraction patterns of 50-nm-thick $Al_{1-x}Mn_xN$ films with varying $x$. For all $x$, ring patterns are observed. This reveals that the $Al_{1-x}Mn_xN$ films are polycrystalline. For $x = 0.05$, diffraction rings derived from würtzite-type AlN $(10\bar{1}0)$, $(0002)$, $(10\bar{1}1)$, $(11\bar{2}0)$, $(10\bar{1}3)$, $(21\bar{3}0)$, $(21\bar{3}1)$, and $(30\bar{3}0)$ are observed. In addition to these rings, for $x = 0.06$ and 0.10, the diffraction rings derived from würtzite-type AlN $(10\bar{1}2)$, $(11\bar{2}2)$, $(20\bar{2}1)$, and $(20\bar{2}2)$ are also observed. For $x = 0.17$, not only the diffraction rings derived from würtzite-type AlN, but also a diffraction ring is observed between the diffraction rings derived from AlN $(10\bar{1}1)$ and $(10\bar{1}2)$. This ring is considered to originate from a secondary phase. Furthermore, for $x = 0.24$, diffraction rings derived from würtzite-type AlN as well as those derived from $ThH_2$-type $Mn_3N_2$ are observed.

First, we discuss the structure of the $Al_{1-x}Mn_xN$ films. For $x$ below 0.10, only würtzite-type AlN phase is confirmed using XRD and TEM observation. However, a possibility of the existence of Mn-rich fine particles below the detection limit of XRD and TEM cannot be excluded completely. For $x = 0.17$, an existence of the secondary phase is observed. The secondary phase might be Al–Mn alloy, Mn-nitrides, or Al–Mn–N ternary compound. Al–Mn alloy forms various phases. Most of these phases show paramagnetism at RT. The Al–Mn alloy containing 0.5–0.6 at. % Mn shows ferromagnetism [13]. For Mn-nitrides,

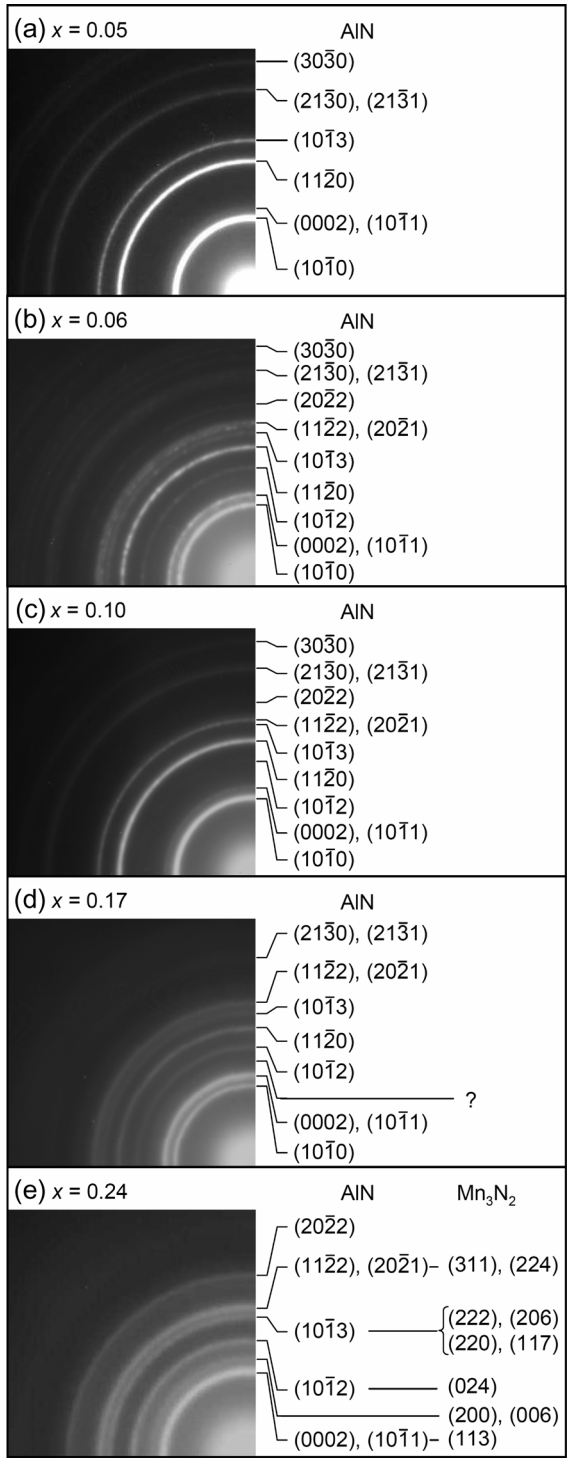


Fig. 4. Selected-area diffraction patterns of 50-nm-thick $Al_{1-x}Mn_xN$ films with various Mn concentrations.

MnN and $Mn_3N_2$ show antiferromagnetism and $Mn_4N$ shows ferrimagnetism [14]. Al–Mn–N ternary compound is not reported. For $x = 24$, it is clear that the $Al_{0.76}Mn_{0.24}N$ film has $ThH_2$-type $Mn_3N_2$ phase, which shows antiferromagnetism with a Neel temperature of 925 K. Finally, we should note that our films are polycrystalline. Thus, the crystalline quality of our films is different from the films grown by MBE [7], which might relate to the difference of magnetic behavior.

Next, we discuss the origin of the magnetic behavior in the $Al_{1-x}Mn_xN$ films from a structural point of view. For $x$ below 0.10, we can consider two possibilities as the origin of paramagnetic behavior; one is Mn ions incorporated into würtzite-type AlN and the other is Mn-rich particles with superparamagnetism [15] below the detection limit of XED and TEM observation. For $x = 0.17$, it is concluded that the magnetic behavior of this film is attributed to the secondary phase. For example, antiferromagetic nanoparticles of NiO and $Cr_2O_3$ are reported to show similar magnetic behavior [16], [17]. Such particles show weak ferromagnetism in low-temperature region. Furthermore, for $x = 0.24$, it is considered that the low magnetization and weak temperature dependence of the dc susceptibility are due to the magnetic behavior of the antiferromagnetic $Mn_3N_2$ phase.

## IV. Conclusion

We have investigated the magnetic behavior and structure of polycrystalline Mn-AlN ($Al_{1-x}Mn_xN$: $x = 0.05$–$0.24$) films with various Mn concentrations $x$. The $Al_{1-x}Mn_xN$ films do not exhibit RT ferromagnetism for all $x$. For $x$ below 0.10, a paramagnetic behavior is observed in the temperature range of 10–300 K. For $x = 0.17$, a magnetic behavior that shows remanent magnetization and coercivity is observed at 10 K. This behavior changes to a paramagnetic one near 20 K as the temperature increases. This magnetic behavior is attributed to the secondary phase described below. For $x = 0.24$, the magnetization is low and the change in dc susceptibility with temperature is small compared with those of films with lower $x$. Only würtzite-type AlN phase is confirmed for $x$ below 0.10. The coexistence of a würtzite-type AlN phase and a secondary phase such as Al–Mn alloy, Mn-nitride, or Al–Mn–N ternary compound is observed for $x = 0.17$. The coexistence of a würtzite-type AlN phase and a $ThH_2$-type $Mn_3N_2$ phase is observed for $x = 0.24$.

## Acknowledgment

This work was supported in part by an Exploratory Research and Encouragement of Young Scientists (B) from the Japanese Ministry of Education, Culture, Sports, Science and Technology (MEXT), Japan. This work was also supported by Priority Assistance for the Formation of Worldwide Renowned Centers of Research—The Global COE Program (Project: Center of Excellence for Advanced Structural and Functional Materials Design) from the Ministry of Education, Culture, Sports, Science and Technology (MEXT), Japan. This work was also supported in part by Strategic Information and Communications R&D Promotion Programme (SCOPE) from the Ministry of Internal Affairs and Communications (MIC). The authors would like to thank Y. Takatsuru, K. Yamamoto, and S. Sato of Rigaku Corporation for performing the grazing-incidence X-ray diffraction analysis.

## References

[1] H. Ohno, H. Munekata, S. Molnar, and L. L. Chang, "New III-V diluted magnetic semiconducors," *J. Appl. Phys.*, vol. 69, pp. 6103–6108, Apr. 1991.

[2] H. Ohno, A. Shen, F. Matsukura, A. Oiwa, A. Endo, S. Katsumoto, and Y. Iye, "(Ga,Mn)As: A new diluted magnetic semiconductor based on GaAs," *Appl. Phys. Lett.*, vol. 69, pp. 363–365, Jul. 1996.

[3] H. Ohno, D. Chiba, F. Matsukura, A. Omiya, E. Abe, T. Dietl, Y. Ohno, and K. Ohtani, "Electric-field control of ferromagnetism," *Nature*, vol. 408, pp. 944–946, Dec. 2000.

[4] A. Oiwa, T. Slupinski, and H. Munekata, "Control of magnetization reversal process by light illumination in ferromagnetic semiconductor heterostructure $p$-(In, Mn)As/GaSb," *Appl. Phys. Lett.*, vol. 78, pp. 518–520, Jan. 2001.

[5] Y. Mitsumori, A. Oiwa, T. Slupinski, H. Maruki, Y. Kashimura, F. Minami, and H. Munekata, "Dynamics of photoinduced magnetization rotation in ferromagnetic semiconductor $p$-(GaMn)As," *Phys. Rev. B, Condens. Matter*, vol. 69, p. 033203, Jan. 2004.

[6] D. Chiba, K. Takamura, F. Matsukura, and H. Ohno, "Effect of low-temperature annealing on (GaMn)As trilayer structures," *Appl. Phys. Lett.*, vol. 82, pp. 3020–3022, May 2003.

[7] R. Frazier, G. Thaler, M. Overberg, B. Gila, C. R. Abernathy, and S. J. Pearton, "Indication of hysteresis in AlMnN," *Appl. Phys. Lett.*, vol. 83, pp. 1758–1760, Sep. 2003.

[8] Y.-Y. Song, P. H. Quang, V.-T. Pham, K. W. Lee, and S.-C. Yu, "Change of optical band gap and magnetization with Mn concentration in Mn-doped AlN films," *J. Magn. Magn. Mater.*, vol. 290–291, pp. 1375–1378, Jan. 2005.

[9] S. Sonoda, S. Shimizu, T. Sasaki, Y. Yamamoto, and H. Hori, "Molecular beam epitaxy of wurtzite (Ga,Mn)N films on sapphire(0001) showing the ferromagnetic behaviour at room temperature," *J. Cryst. Growth*, vol. 237–239, pp. 1358–1362, Apr. 2002.

[10] Y. Endo, T. Sato, A. Takita, Y. Kawamura, and M. Yamamoto, "Magnetic, electrical properties and structure of Cr-AlN and Mn-AlN thin films grown on Si substrates," *IEEE Trans. Magn.*, vol. 41, pp. 2718–2720, Oct. 2005.

[11] T. Kondo, S. Kuwabara, H. Owa, and H. Munekata, "Molecular beam epitaxy of (Ga,Mn)N," *J. Cryst. Growth*, vol. 237–239, pp. 1353–1357, Apr. 2002.

[12] L. Neel, "Some new results on antiferromagnetism and ferromagnetism," *Rev. Mod. Phys.*, vol. 25, pp. 58–63, Jan. 1953.

[13] P. C. Kuo, Y. D. Yao, J. H. Huang, S. C. Shen, and J. H. Jou, "Microstructural and magnetic studies of Mn-Al thin films," *J. Appl. Phys.*, vol. 81, pp. 5621–5623, Apr. 1997.

[14] M. Tabuchi, M. Takahashi, and F. Kanamaru, "Relation between the magnetic transition temperature and magnetic moment for manganese nitrides $MnN_y$ $(0 < y < 1)$," *J. Alloys Comp.*, vol. 210, pp. 143–148, Aug. 1994.

[15] R. H. Kodama, "Magnetic nanoparticles," *J. Magn. Magn. Mater.*, vol. 200, pp. 359–372, Oct. 1999.

[16] S. A. Makhlouf, F. T. Parker, F. E. Spada, and A. E. Berkowitz, "Magnetic anomalies in NiO nanoparticles," *J. Appl. Phys.*, vol. 81, pp. 5561–5563, Apr. 1997.

[17] M. B. Lopez, C. V. Vazquez, J. Rivas, and M. A. L. Quintela, "Magnetic properties of chromium (III) oxide nanoparticles," *Nanotechnology*, vol. 14, pp. 318–322, Jan. 2003.

Manuscript received February 27, 2008. Current version published December 17, 2008. Corresponding author: T. Sato (e-mail: takanobu.sato@mat.eng.osaka-u.ac.jp).